JOURNAL OF CATALYSIS 156, 243–254 (1995)

XPS and NO Adsorption Studies on Alumina-Supported Co–Mo Catalysts Sulfided by Different Procedures

L. Portela,[1] P. Grange, and B. Delmon[2]

Unité de Catalyse et Chimie des Matériaux Divisés, Université Catholique de Louvain, 2/17, Pl. Croix du Sud, B-1348 Louvain-la-Neuve, Belgium

Received October 14, 1994; revised March 17, 1995; accepted June 20, 1995

In the present work we studied the distribution of the active phase at the surface of the support, by XPS, of four HDS catalysts, each of them sulfided according to five different procedures. The procedures employed were known to yield catalysts with distinct activities and selectivities. The results of the XPS study were refined with data from an IR study on NO adsorbed on the catalysts. The major consequence of the modification of the activation procedure was a change in the dispersion of the active phase rather than the modification of the oxidation states of the active elements. The diameter of the MoS_2 crystallites, rather than the number of slabs per crystallite, was most affected. When H_2S was employed in the absence of hydrogen, catalysts containing only Mo contained a large excess of surface sulfur, whereas Co–Mo catalysts still presented S/Mo XPS ratios close to the stoichiometric ones. In these activations, the NO adsorption capability of the catalysts depended on whether the H_2S treatment was applied before or after the sulfidation with H_2/H_2S.

INTRODUCTION

The modification of the activation (sulfidation) procedure is known to yield hydrodesulfurization (HDS) catalysts with markedly different catalytic performances, even when only H_2 and H_2S are used in various sequences (1–6). The interesting aspect in using different activation procedures is that one ends up with catalysts showing different behaviours albeit having all the same active phase loading, since they were obtained from the *same oxidic precursor.* This way it should be possible to detect the characteristics needed for a good HDS catalyst and, maybe, to get further insight into the nature of its active sites. The present work is based on and is an extension of previous investigations on the same line carried on in our laboratory (4, 7).

XPS studies of oxidic Mo-containing HDS catalysts have shown that Mo atoms are usually found in a (VI) oxidation state, corresponding to an MoO_3 phase. For alumina-supported catalysts, it is commonly accepted that up to a loading of about 15–20 wt% of MoO_3, Mo exists as an ordered or patch-like layer of MoO_3, and that above that loading bulk-like MoO_3 crystallites begin to form (8–10). Many authors point to the patch-like distribution as the most probable one (11–15). Okamoto and co-workers (10) mentioned two different environments for the Mo atoms in the freshly prepared oxide catalyst. At high Mo loading (>20 wt% MoO_3) octahedral polymeric Mo(VI) is formed, with a structure and properties similar to those of bulk MoO_3. At lower loading, tetrahedral Mo(VI) species in higher interaction with the support may be found. Some authors still divide the latter category into monomeric tetrahedral molybdena and dimeric tetrahedral molybdena (8, 9).

The three previously mentioned Mo species have different responses to reducing and sulfiding treatments. By XPS it was found that octahedral Mo(VI) could be reduced and sulfided to Mo(IV). Monomeric tetrahedral Mo would be very hard either to reduce or sulfide. Dimeric tetrahedral Mo species could be reduced, with hydrogen, only down to a (V) oxidation state, whereas upon sulfidation with a hydrogen/hydrogen sulfide mixture a (IV) oxidation state could be reached (8, 9). The existence of Mo(V) in sulfided Mo/Al_2O_3 catalysts was confirmed by ESR (16).

At the surface of Co-containing, freshly prepared, alumina-supported catalysts, two main types of Co environments were identified by XPS: a cobalt oxide environment, where Co exists as Co^{2+}, though at higher loading Co_3O_4 starts to form, as confirmed by Leyrer *et al.* (17); and a pseudo-cobalt aluminate (18–24). In Co–Mo catalysts, the order of Co insertion may also influence the location and type of phases formed by Co. In an insertion after Mo, it is suggested that an interaction between Co and Mo oxide phases exists (20 and references therein, 26, 27). In this Co–Mo interaction phase, Co exists as a layer between the Mo layer and the Al carrier (22, 28, 29). The interaction of Co with Mo would prevent the formation of Co–Al

[1] Present address: GRECAT—Dep. Eng. Química, Instituto Superior Técnico, Universidade Técnica de Lisboa, Av. Rovisco Pais, P-1096 Lisboa Codex, Portugal.

[2] To whom correspondence should be addressed.

0021-9517/95 $12.00

interaction species. This could explain the increased surface concentration and dispersion of Co in bimetallic catalysts, compared to single-metal ones. In the Co–Al interaction species, Co can exist in two types of locations: octahedral ones and tetrahedral ones (25, 30). Their reactivities differ during sulfidation of the catalyst; the former is supposed to be the most reactive species (30).

The sulfidation of Co oxide produces mainly Co_9S_8, and its reduction yields metallic cobalt. Since the XPS peak positions of the metallic and sulfided cobalt are very close to each other, it is not easy to decide whether or not Co^0 is present in the sulfided catalyst. However, considering its easy sulfidation under the usual activation conditions, with H_2/H_2S, one can safely exclude the presence of the metallic form (31).

Mössbauer emission spectroscopy (MES) studies showed that, in the presence of Mo, cobalt could exist in a sulfided environment distinct of all known Co sulfided phases (11). The structure of Co in this new Co–Mo interaction phase is not clear. It is generally accepted that Co atoms lie on the edges of the Mo sulfide crystallites (32). However, a similar MES Co signal was found when low loading carbon-suppported Co catalysts containing no molybdenum were sulfided (33). This special configuration of sulfided cobalt yields an XPS signal nearly in the same position as that of Co_9S_8, thus not permitting a good differentiation using this technique (11). During actual catalytic work, under industrial conditions, the MES signal was shown to disappear yielding the normal Co_9S_8 signal (34).

Since in the *freshly activated* state the catalysts are always composed of Co_9S_8, MoS_2, and Co-decorated MoS_2 (35–42), the differences in the final activity must rely upon their distribution at the surface of the support and on the concentration of active sites issuing from a certain activation protocol.

EXPERIMENTAL

Catalysts

In the present work we used three home-made catalysts and an industrial one. The latter was an industrial γ-alumina-supported bimetallic Co–Mo, the HR-306 from Procatalyse. It had a BET surface area of 195×10^3 m^2/kg and the following composition: 2.7 wt% of cobalt, as CoO, and 13.5 wt% of molybdenum, as MoO_3, as determined by atomic absorption spectroscopy.

Preparation

The support used in the preparation of the catalysts was a γ-Al_2O_3 from Rhône–Poulenc, with a BET surface area of 234×10^3 m^2/kg and a total pore volume of 0.61×10^{-3} m^3/kg. The original extrudates were cylindrical, 1×10^{-3} m diameter by 6×10^{-3} m long, and were ground and sieved to a size between 0.315×10^{-3} and 0.500×10^{-3} m before any impregnation. It was calcined in a tubular reactor under a flow of dry air (Air Liquide) at 773 K overnight.

Mo/γ-Al_2O_3. This catalyst was prepared using the pore-filling method in two steps, using a solution of ammonium heptamolybdate tetrahydrate (Merck, p.a.). The solution, with a pH around 5 (43), was poured over the support and the whole mixed with a spatula until no inhomogeneities could be observed. The impregnated, wet alumina was dried at 367 K in a tubular reactor under a flow of dry air (Air Liquide) overnight. A second impregnation, under similar conditions, was then performed. Afterwards the dry material was calcined at 773 K for 2 h, also under a flow of dry air. Its Mo content was 15.1 wt% MoO_3, as determined by atomic absorption spectroscopy.

Co/γ-Al_2O_3. This catalyst was prepared by wet impregnation of the support (0.05 kg) with 0.2×10^{-3} m^3 of a solution of cobalt nitrate hexahydrate (Merck, p.a.) with appropriate concentration. The solvent (water) evaporation took place under constant stirring and vacuum (water pump) at ambient temperature in a rotary evaporator until the solid seemed completely dry (when the grains didn't stick together). It was further dried and calcined like the Mo catalyst. The Co content was 2.9 wt% Co as CoO, determined by atomic adsorption spectroscopy.

CoMo/γ-Al_2O_3. For the preparation of the CoMo catalyst we used the previously prepared Mo catalyst and impregnated it with 0.2×10^{-3} m^3 of a solution of cobalt nitrate hexahydrate (Merck, p.a.) in water (23 vol%) and ethanol (Carlo Erba R.P.E., 77 vol%) with appropriate concentration. Since MoO_3 is almost insoluble in ethanol, the danger of its redissolution during the cobalt impregnation is largely reduced, and the initial architecture of the Mo catalyst is better preserved (44). Any differences in the Mo structure after calcination can, thus, be ascribed to the presence of Co and not to any rearrangement during the impregnation step of the latter. The Co impregnation was performed as in the case of the Co/γ-Al_2O_3 catalyst. The Co and Mo contents, as determined before, were 3.1 wt% CoO and 14.9 wt% MoO_3.

The BET surface area (1-point method) was measured for all calcined catalyst. The values obtained were in the range of $195–210 \times 10^3$ m^2/kg.

Activation

The catalysts were activated (sulfided) according to five different procedures:

(i) Simultaneous reduction and sulfidation with a mixture of H_2/H_2S (15 vol%) at 1.67×10^{-6} m^3/s. Activation named RS.

(ii) Pre-reduction (R) with hydrogen at 1.67×10^{-6}

m^3/s, followed by simultaneous reduction/sulfidation (RS) as above. Activation named R/RS.

(iii) Pre-sulfidation (S) with a mixture of H_2S (15 vol%)/Ar, at 1.67×10^{-6} m^3/s, followed by simultaneous reduction/sulfidation as in (i). Activation named S/RS.

(iv) Initial simultaneous reduction/sulfidation, as in (i), followed by reduction, as in the first part of (ii). Activation named RS/R.

(v) Initial simultaneous reduction/sulfidation, as in (i), followed by sulfidation, as in the first part of (iii). Activation named RS/S.

In all activations the catalyst (oxide form) was first heated to 423 K at 0.17 K/s under a flow of Ar and remained at that temperature for half an hour. Afterwards, the activation gases were introduced and the temperature rose, at the same rate, up to 673 K where it remained for 1 h. In the case of double step activation procedures (cases (i) to (v)), after the first hour the gases were switched to the mixture corresponding to the second step and the temperature was maintained for another similar period of time.

The gases were all supplied by Air Liquide, and purity was 99.90% for H_2; 99.0% for H_2S, and 99.995% for Ar. The last was further purified by flowing, at room temperature, through an activated 4 A molecular sieve to remove water, and through an Oxy-Trap (Alltech Associates) to remove any traces of oxygen. After the activation, the catalysts were transferred into flasks containing iso-octane (Merck, p.a., used as received), without being exposed to air.

XPS Analyses

For the XPS analysis, each catalyst was pressed at 3000 kg, with a polyacetal cylinder, onto a stainless-steel sample holder (6×10^{-3} m diameter). To avoid any contact with air during its transfer from the container to the sample holder (for pressing) and from the latter into the preparation chamber of the spectrometer, the surface of the catalysts was protected by a meniscus of iso-octane (UCB, used as received). The latter was evaporated during the pumping in the chamber (overnight, final pressure of approx. 7×10^{-5} Pa).

The spectrometer used was a Surface Science Instruments SSX-100, Model 206 with a monochromatic Al$K\alpha$ source (1486.6 eV), operating at 10 kV and 15 mA. The spectrometer was interfaced to a Hewlett–Packard 9000/310 computer for data acquisition and treatment. The sample holders were mounted on an insulated Teflon base to avoid peak duplication, due to differences between the conductivity properties of the support and the sulfided active phase (MoS_2 is a semi-conductor and alumina is an insulator). The sample holders were also covered with a nickel grid placed at 3×10^{-3} m above its surface. We compensated the positive charge developed on the samples, due to electron ejection, with an electron floodgun operating at 6 eV. The pressure in the analysis chamber was about 4×10^{-7} Pa during analysis.

We performed all of the analysis in the "constant pass energy" mode, with a pass energy of 150 eV. The lines O1*s*, Al2*p*, S2*p*, Mo3*d*, and Co2*p* were investigated, always in the same sequence, and the binding energy (BE) values were reported to the C1*s* line at 284.8 eV, corresponding to carbon in C–H or C–C environments. This carbon is probably a contamination from residual iso-octane. We checked this line at the beginning and after the analysis of each catalyst and couldn't find any modification in its position. Under the operative conditions of the analysis the precision of the BE values was 0.16 eV.

The intensity of the peaks was taken as the area beneath the curves down to a nonlinear, Shirley-type (45) baseline. Surface atomic concentration ratios were calculated as the ratio of the corresponding peak intensities, corrected with theoretical sensitivity factors based on Scofield's photoionisation cross sections (46).

The S2*p* and Mo3*d* lines (the latter contained the S2*s* line in the envelope, which had to be removed for quantitative analysis) were decomposed using an iterative least-squares computer program, the curves being taken as 85% Gaussian and 15% Lorenzian. In the decomposition of the Mo3*d* peak envelope several constraints were imposed to give physical significance to the peaks thus obtained:

(i) 3.15 eV for the spin–orbit splitting of the Mo3*d* peak (distance between the $Mo3d_{5/2}$ and the $Mo3d_{3/2}$ peaks), independently of the oxidation state of Mo (obtained from pure compounds, MoO_3 and MoS_2 both supported and bulk);

(ii) the $Mo3d_{5/2}/Mo3d_{3/2}$ area ratio was kept constant and equal to the theoretical value of 1.5 (Ref. 47, p. 113);

(iii) the full width at half maximum (FWHM) of the $Mo3d_{5/2}$ and $Mo3d_{3/2}$ peaks of the Mo(V) and Mo(VI) oxidation states were kept equal to the corresponding ones of the Mo(IV) oxidation state (the latter predominated in the sulfided catalysts, thus yielding well defined peaks). This had to be assumed since, due to peak overlapping, it was not possible to clearly determine the individual widths.

After preliminary decomposition of the sulfided catalysts' Mo3d peaks, the results showed that excessive FWHM and unacceptable peak positions would be obtained if only two Mo oxidation states were considered, either (IV) and (VI) or (IV) and (V); therefore, in that decomposition we considered the three possible oxidation states in that situation, i.e., Mo(IV), (V), and (VI). There was no need to consider metallic Mo in any of the catalysts.

Nitric Oxide Adsorption

First, the activated catalysts were ground and then wafers weighing between 5 and 8×10^{-6} kg were made having

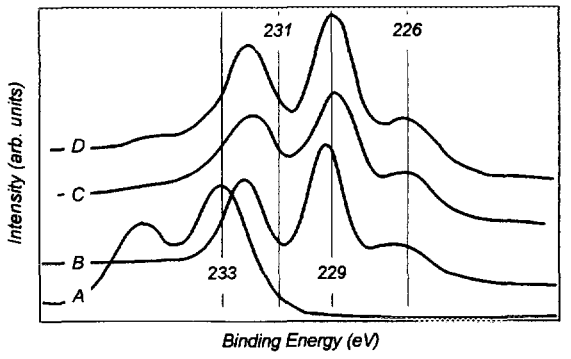

FIG. 1. XPS spectra (Mo3*d* level) of the oxidic Mo catalyst (spectrum A) and of the S/RS-activated catalysts: (B) Mo; (C) CoMo (lab.), and (D) CoMo (ind.).

a diameter of 1.3×10^{-2} m. In the case of two-part activations, only the first part was performed before grinding, and only the second part was performed inside the IR cell. For the measurement of the IR spectra we used a tailor-made cell which allowed the activation of the catalysts, the NO adsorption, and the IR measurements, without any contact with the laboratory's atmosphere.

The NO adsorption was performed at ambient temperature, at 4 KPa of purified NO (Air Liquide, 99.9% nominal purity). The spectra were taken with a Fourier Transform Infrared Spectrometer, Brüker IFS-88, interfaced to a Brüker proprietary computer system for data processing.

For semi-quantitative purposes, we considered the intensity of the bands of adsorbed NO as the height of selected peaks down to a linear baseline. For the adsorption on Co we used the symmetric stretching vibration peak, around 1850 cm^{-1}, and for the adsorption on Mo we used the antisymmetric stretching vibration peak, around 1700 cm^{-1}. These are the two bands which do not overlap in the case of bimetallic catalysts. All intensities were normalised to a constant wafer weight. Full details of the experimental procedure can be found elsewhere (48).

RESULTS

XPS

Peak Position and Line Broadening

For the sake of simplicity in Figs. 1, 2, and 3 we only present the most representative spectra of each class of catalysts. All differences due to other activations are mentioned in the text.

Molybdenum and sulfur. In Fig. 1 one can see the changes induced on the Mo phase of the catalysts upon sulfidation. Spectrum A shows the Mo3*d* doublet of the oxide phase of the Mo catalyst (the spectra of the corresponding CoMo catalysts are similar to this one) with a position that is characteristic of Mo(VI), normally MoO_3 (ca. 233 eV for the Mo3$d_{5/2}$ peak). No components that may be attributed to other oxidation states are present.

Upon sulfidation (spectra B through D), the peaks corresponding to the Mo(VI) species almost disappear, yielding others at a lower binding energy level. These new peaks are attributed to a Mo(IV) species (ca. 229 eV) and, to a less extent, to a possible Mo(V) species (ca. 231 eV). Furthermore, one can remark the appearance of a peak characteristic of the 2*s* level of S^{2-} (ca. 226 eV). Simultaneously, another band appears around 162 eV (see Fig. 2) corresponding to the 2*p* level of the same species.

In the case of both CoMo catalysts, in Fig. 1, one can observe the presence of a weak and broad shoulder in a position corresponding to that of the Mo3$d_{3/2}$ peak of the oxidic catalyst. This shoulder is nearly absent in the Mo/Al_2O_3 catalyst in any of the activations considered. Also, the peak between 231 and 233 eV is broader in the case of the bimetallic catalysts.

The Mo(IV) species produced under the conditions of the activation procedures employed corresponds normally to an MoS_2 phase, stoichiometric or not. It is not possible, using XPS, to distinguish between oxidised and sulfided Mo(IV). Therefore, if the sulfidation was not complete, the observed Mo3*d* envelopes would contain a contribution from the former species. Mo(IV) oxysulfide phases also would yield peaks in the same position. In Table 1 we show the positions of the Mo3*d* and S2*p* peaks and the widths of the Mo3*d* peaks of all the catalysts analysed in their oxide and activated forms (where applicable).

The position of the different Mo lines did not change significantly with the different activation procedures. The dispersion of the values is larger for the Mo(IV) oxidation state. This can be explained by the very low amount of Mo atoms found in this state, which makes the curve fitting very difficult and less precise in the region of higher binding energies. The values agree, however, with those present in the literature (8, 18, 49, 50). The activation of the catalyst,

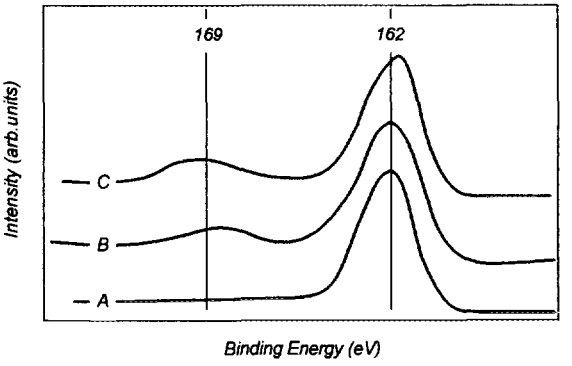

FIG. 2. XPS spectra of the S/RS-activated catalysts (level S2*p*): (A) Mo; (B) CoMo (lab.); and (C) CoMo (ind.).

TABLE 1

Position and Widths of the Mo and S Peaks

Catalyst	Activ.	S^{2-} (eV)	Mo3$d_{5/2}$(eV)			
		S2$p_{3/2}$	Mo(IV)	Mo(V)	Mo(VI)	FWHM[a]
Mo	Oxide	—	—	—	233.2	2.5
	S/RS	162.1	229.2	—	—	1.6
	R/RS	161.9	229.1	230.9	232.6	1.9
	RS	162.1	229.1	231.0	232.7	1.7
	RS/S	162.3	229.4	231.1	232.5	1.5
	RS/R	162.0	229.1	230.8	232.6	1.7
CoMo (lab.)	Oxide	—	—	—	233.0	2.4
	S/RS	161.7	228.8	230.8	233.0	1.9
	R/RS	161.9	229.0	230.9	232.6	1.8
	RS	161.9	229.0	231.1	232.8	1.8
	RS/S	161.9	229.1	231.0	233.0	1.9
	RS/R	162.0	229.1	230.9	232.9	1.8
CoMo (ind.)	Oxide	—	—	—	232.7	2.5
	S/RS	162.1	229.0	230.8	232.9	1.8
	R/RS	162.1	229.1	230.8	232.8	1.7
	RS	162.1	229.1	230.8	233.0	1.9
	RS/S	162.1	229.2	230.8	232.7	1.7
	RS/R	162.0	228.9	230.7	232.7	1.6

[a] FWHM of the Mo3$d_{5/2}$ peaks of all Mo species considered. See the Experimental Section.

independently of the procedure used, produces a very marked decrease in the FWHM of the Mo band. Generally, both Co–Mo catalysts present FWHM slightly larger than the Mo one.

A higher dispersion of the values corresponding to the S2*p* peak position was also found. The existence of elemental-like sulfur species at the surface of the catalyst is possible. However, the resolution mode of the spectrometer used in this work and the relative closeness of the sulfur bands corresponding to the S^{2-} and S^0 states (163.7 and 161.9 eV, respectively, (18)) do not allow a precise decomposition of the S2*p* envelope. Since the former species is certainly predominant (the maxima of the different envelopes agree well with that hypothesis), the whole band was assigned to it. In both Co–Mo catalysts, a new sulfur band at 169 eV is present, corresponding to a sulfate species (Fig. 2, spectra B and C). Its absence in the Mo catalyst and the easy oxidation of Co sulfide (21, 51) suggest that it belongs to Co sulfate.

The S2*p* peaks detected in the Co catalysts were very weak and broad so that neither their position nor their intensity could be reliably quantified. Therefore, we do not include that data in Table 1.

Cobalt. In Fig. 3 we represent the Co2*p* bands of the Co catalyst and of the industrial one in selected conditions. No peak decomposition was performed here due to the very low intensity of the Co signal, the existence of several peaks for each species (main ones and satellites), and the uncertainty with regard to the correct positioning of the baseline.

All Co-containing catalysts in the oxide form yielded spectra similar to that of Fig. 3A. The spectra presented the 2$p_{3/2}$ peak around 781.5 eV and the 2$p_{1/2}$ peak around 797 eV. The distance between these two peaks lies between the one characteristic of paramagnetic Co species (16 eV, cobaltous compounds) and diamagnetic species (15 eV, cobaltic compounds) (16, 22).

Another peak, corresponding to shake-up processes, can be found between the aforementioned ones, at 787 eV. Its broadness doesn't allow a precise attribution of the binding energy value, and therefore a distinction between Co^{2+} ions in different configurations (tetrahedral—difference in BE between this peak and the Co2$p_{3/2}$ equal to 5.3 eV; and octahedral—difference in BE equal to 6.2 eV) is not possible. The broadness of the latter band is an indication that several types of species may be present. However, since Co(III) compounds, such as Co_2O_3, present a weak and broad satellite at energies higher than the ones detected in the present spectra, the peaks observed are tentatively attributed to CoO and/or $CoAl_2O_4$ (16).

Upon sulfidation a new peak around 779 eV appears for all catalysts, corresponding to a metallic or sulfided form of Co. Under the present activation conditions, the sulfided form is more likely to exist than the metallic one.

For the Co catalyst, the remaining activations yielded spectra with shapes between those of Fig. 3, spectra B and C. Both Co–Mo catalysts yielded similar spectra in similar activations. In the cases of the S/RS and RS/S activations

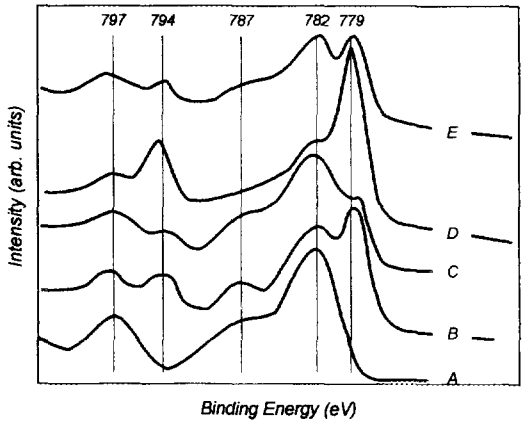

FIG. 3. Co2*p* peaks of the Co-containing catalysts: (A) oxidic Co catalyst; (B) Co catalyst activated according to RS/S; (C) Co catalyst activated according to RS/R; (D) CoMo catalyst (ind.), as in (B); and (E) CoMo catalyst (ind.) as in C).

TABLE 2

XPS Peak Intensity Ratios for the Oxide and Activated Catalysts

	Catalysts								
	Mo		Co	Co–Mo (lab.)			Co–Mo (ind.)		
Act.	Mo/Al	S/Mo	Co/Al	Mo/Al	Co/Al	S/Mo	Mo/Al	Co/Al	S/Mo
Oxide	0.077		0.016	0.075	0.032	—	0.074	0.026	—
S/RS	0.031	3.9	0.010	0.067	0.029	2.2	0.058	0.018	2.2
R/RS	0.071	1.6	0.011	0.078	0.020	1.8	0.072	0.023	1.8
RS	0.067	1.9	0.010	0.076	0.026	1.9	0.058	0.018	1.9
RS/S	0.041	3.6	0.009	0.072	0.025	2.6	0.072	0.024	2.2
RS/R	0.055	1.8	0.010	0.075	0.023	2.0	0.065	0.019	1.7

they were close to that depicted in Fig. 3, spectrum D, whereas in the remaining cases they were like the one presented in Fig. 3, spectrum E.

Peak Intensity Ratios

In Table 2 we present the results of the elemental analysis of the catalysts. The values represent the ratio of normalised XPS peak intensities and correspond to surface atomic ratios.

After mathematical decomposition of the Mo3*d* peak envelope in sulfided samples, it was possible to conclude that more than 82% (more than 87% for the Mo catalyst) of the original Mo(VI) was converted to lower oxidation states, of which Mo(IV) was, by far, the most abundant.

The results of Table 2 confirm that the activation procedures always influence the dispersion of Co and Mo on the surface of the catalysts. In a general way, Mo/Al ratios are higher in the oxide catalysts than in the activated ones. This indicates a better coverage of the support by the Mo phase. For a given activation procedure it is observed that the two Co–Mo catalysts present Mo/Al ratios usually higher than those of the Mo catalyst. The Mo/Al relative variations, from one activation to another, remain similar for all of them, though more pronounced in the Mo catalyst, for which a wider range of values is observed. The highest Mo/Al ratio is always obtained with the R/RS treatment.

For a certain catalyst, the relative intensities of the peaks corresponding to the sulfided and oxidised forms of Co are very sensitive to the activation procedures (see Fig. 3). As a rule, the relative intensity of the peak corresponding to a Co sulfide species is higher in the Co–Mo catalysts (Fig. 3, spectra D and E) than in the Co one (Fig. 3, spectra B and C). Within each category of catalysts, that peak is more intense for the activations where, at some stage, H_2S was used in the absence of hydrogen, the S/RS and RS/S activations (Fig. 3, spectra B and D).

Similarly to what happened to the Mo/Al ratio, the Co/Al ratio also decreases after sulfidation. The influence of the activation procedure is less important in the Co catalyst, for which the Co/Al ratio in the sulfided catalysts remains nearly constant. However, when dispersed over Mo, in the two Co–Mo catalysts, there is a significant increase of Co present at the surface, often more than twice as much as in the Co catalyst. This is a confirmation of previous work done in this laboratory (7, 26). Furthermore, the dispersion of Co in the latter case becomes more sensitive to the activation procedures. In the two Co–Mo catalysts, the industrial one usually presents lower Co/Al ratios, and the response of the latter to the activation procedures is different from that of the laboratory prepared catalyst.

In Table 2 it is possible to see that the amount of sulfur present at the surface (expressed as the S/Mo ratio) is also sensitive to the activation procedure but, apart a few exceptions, it is close to the stoichiometric value (S/Mo = 2). Its relative variations are approximately the same for the Mo-containing catalysts although they are more marked in the Mo catalyst. The ratio is maximal when H_2S was used in the absence of hydrogen at a certain stage of the activation (S/RS and RS/S). For the Mo catalyst these two procedures yield S/Mo ratios well above the stoichiometric ratio, contrary to what happens with the Co/Mo ones.

IR Study of Adsorbed Nitric Oxide

The IR spectrum of NO absorbed on the activated catalysts showed the usual doublets in the case of Mo and Co catalysts and triplets in the case of both bimetallic catalysts, as shown in a typical case, that of the RS-activated catalysts, in Fig. 4. In case of differences with other activation procedures, they will be indicated in the text. The position of these bands agrees with literature data (3, 52). In a previous work (53) we have shown that the intensity of the bands of adsorbed NO was affected by the activation procedures.

Treating an already activated catalyst with H_2S at 673 K,

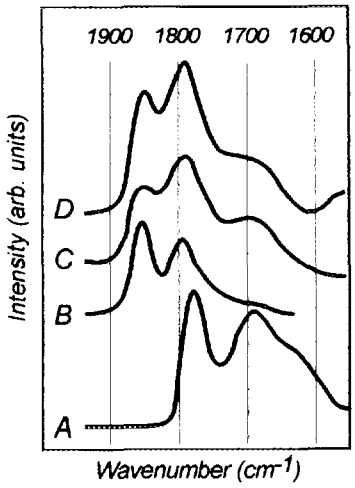

FIG. 4. IR absorbance spectra of NO adsorbed on sulfided (RS) catalysts: (A) Mo; (B) Co; (C) Co–Mo (lab.); and (D) Co–Mo (ind.).

as in the RS/S activation, leads to a negligible NO adsorption either on Co or on Mo. In contrast, if the H_2S treatment is applied to the oxidic catalyst, followed by the usual H_2/H_2S treatment (S/RS activation), the NO adsorption takes place in a way similar to the case of other activations. This is valid for all catalysts. The sulfur content in the Mo catalyst after the S/RS and RS/S activations can be almost twice as high as in both bimetallic ones (see Fig. 5).

To evaluate the influence of the sulfided metals' dispersion on the amount of adsorbed NO, we considered the modification of the intensity of the bands of adsorbed NO as a function of the *M*/Al XPS ratio (*M* = Mo and Co). The two bimetallic catalysts showed no special relationship between the two parameters, whereas the two monometallic catalysts presented a proportional increase of the amount of adsorbed NO as the *M*/Al ratio increased (see Fig. 6). However, the change in Co dispersion was much smaller than the corresponding change in Mo dispersion. This is to be emphasized, as *the data in both plots of Fig. 6 correspond to the same Mo and Co oxidic precursors activated according to different procedures, and not to catalysts with a changing active phase loading.*

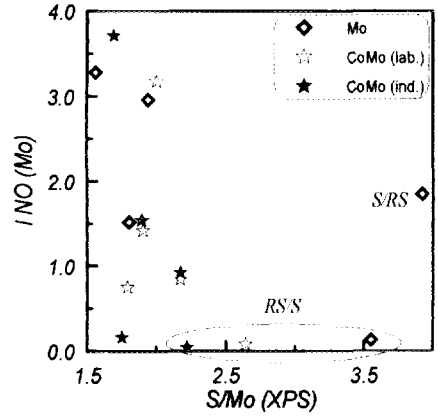

FIG. 5. Intensity of the bands of NO adsorbed on Mo as a function of the surface sulfur content of the catalysts.

DISCUSSION

Chemical and Textural Transformations Occurring during Activation

Molybdenum. The main Mo phase present after sulfidation appears to be sulfided Mo(IV) (see Figs. 1 and 4 and Table 1), with a stoichiometry close to MoS_2 (see Table 2). The existence of Mo(VI) after the activation is a sign that the sulfidation wasn't complete. It should correspond to Mo atoms in a strong interaction with the support, the sulfidation of which occurs only at temperatures higher than the ones presently employed (8, 9). The decrease of the Mo peaks FWHM after activation is a sign of the decrease of interaction of the Mo phase with the support.

After sulfidation, the percentage of Mo present as Mo(IV) lies between 72 and 100. This agrees with the results of Zingg *et al.* (8), who proposed that, in the oxide phase and for a Mo loading of 15% MoO_3 (the case of our catalysts), about 72% of the Mo atoms will exist in octahedral coordination whereas the remainder will be in tetrahedral coordination. The reduction/sulfidation behaviour of these two species was mentioned in the introduction.

The general decrease of the Mo/Al atomic ratios when passing from the oxide to any sulfided state (especially in the case of the monometallic catalysts), as shown in Table 2, is a direct consequence of the structural changes undergone by the Mo phase upon sulfidation, the loss of dispersion associated with the transformation of MoO_3 patches or monolayer into tridimensional MoS_2 crystallites, and the higher exposure of Al atoms in that situation. This effect was also observed by other authors (10, 54) and is a confirmation of previous work done in our laboratory (55).

The results presented in Fig. 6A allow us to draw some conclusions with regard to the significance of the variation of the dispersion indicator, the Mo/Al XPS ratio, as a consequence of the different activations, in the case of the monometallic Mo catalyst. A variation of the Mo/Al ratio from one activation to another means that the coverage of the surface of the support by the Mo-containing phase has changed. Since we are dealing with catalysts with a constant Mo loading this implies that either the diameter of the MoS_2 crystallites has changed (leading to a variation of the total edge area) or that the number of slabs per crystallite has changed (the total edge area remains unchanged in this situation). In the first case the total amount of NO should change as well, since it is known that NO

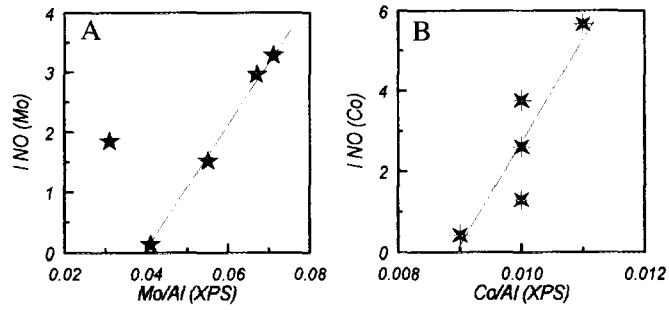

FIG. 6. Modification of the NO uptake as a function of the active phase dispersion: (A) Mo catalyst and (B) Co catalyst.

adsorption sites are formed preferably at the edges of MoS_2 crystallites (where S species are more labile (56)), whereas in the latter case the total amount of adsorbed NO should remain constant. The results of Fig. 6A indicate that it is the diameter of the MoS_2 crystallites that is affected when the activation procedure changes. The only case suggesting a different explanation corresponds to the R/RS activation, after which the sulfidation may be incomplete: this point will be discussed later. The lack of any correlation in the cases of both bimetallic catalysts is an indication of a mutual interference between Mo and Co.

Cobalt. The general decrease of the Co/Al ratio suggests that the sulfidation of the Co oxide phase is accompanied by sintering. This is true for the Co catalyst and for both Co–Mo ones. However, in the latter, the presence of Mo prevented a decrease as deep as with the monometallic catalyst in agreement with what was mentioned in the introduction.

The remarkable increase of the Co surface concentration (Co/Al ratio), upon inserting it in an Mo catalyst, shows that Mo diminishes the interaction between Co and the support, thus inhibiting the migration of the former into subsurface positions to form nonsulfidable species. In fact, several authors (25, 26, 57) confirmed that the presence of Mo in the catalyst increased the fraction of extractable Co in an alumina-supported Co–Mo catalyst. The higher intensity of the XPS peaks corresponding to sulfided Co species, shown in Fig. 3, is a confirmation of this hypothesis. Since the increase of the surface concentration of Co, in the Co–Mo catalysts, is first seen in the oxide phase, as was observed by other authors (25, 26), an interaction between the Co and Mo phases probably occurs there. This higher sulfidable Co concentration should be the cause for the higher sensitivity of the Co/Al ratio to the activation procedures in the bimetallic catalysts seen in Table 2. The higher Co/Al ratio found in bimetallic catalysts cannot be attributed to a more extensive coverage of the support, when compared to the monometallic ones, since the intensity of the Al peaks was virtually the same in all catalysts analysed.

The results of Fig. 6B indicate that the size of the Co_9S_8 crystallites is also affected when the activation procedure is changed. As had happened in the case of Mo, the proportional increase of the amount of adsorbed NO as the Co/Al ratio increases is no longer verified in the case of the bimetallic catalysts, confirming again the mutual interference between Co and Mo in bimetallic catalysts.

An apparent contradiction exists between the results obtained in the present work and those of Gajardo *et al.* (25). Those authors proposed that when Co is inserted alone in the alumina support, due to the poor dispersion obtained, no pseudo-cobalt aluminate is produced, and instead only Co_3O_4 is observed. On the other hand, if Mo is present at the surface of the supported, an increased dispersion is observed and $CoAl_2O_4$ starts to form. This fact was attributed to the high Co dispersion, favouring the interaction of the latter with the support and consequently the formation of the aluminate. Our XPS results point to the formation of the nonsulfidable and nonreducible $CoAl_2O_4$ in both monometallic and bimetallic catalysts. The amount of this species appears to decrease when Mo is present in the catalyst prior to the Co insertion.

This difference of behaviour can be attributed to the impregnation methods used in the two studies. Gajardo *et al.* (25) used the pore filling method. This method was shown to produce poor active element dispersions, even when an easy impregnable metal such as molybdenum was considered (12). Thus the explanation proposed by the authors to account for the absence of $CoAl_2O_4$ could be correct: the agglomeration of Co would prevent an efficient contact with the support, and therefore minimise the aluminate formation. The higher dispersion induced by the presence of molybdenum would be responsible for the appearance of that compound in the bimetallic catalysts. In our case, the wet impregnation must have provided a better, because more homogeneous, contact between the active element and the support, leading to a dispersion increase and to the formation of pseudo-Co aluminate. The presence of Mo at the surface of the catalyst, by preventing such a deep interaction between Co and the support, would have decreased the amount of $CoAl_2O_4$ formation.

In all catalysts analysed, the sulfidation of the Co phase seemed favoured by treatments where H_2S was employed in the absence of H_2 (S/RS and RS/S), as seen in Fig. 3. Steinbrunn and Bordignon (58) and Dumas *et al.* (59) observed that the sulfidation of CoO single crystals, with either H_2S or H_2/H_2S, proceeded via the initial formation of flat, smooth islands of metallic Co, covered by sulfur layers. The sulfidation of these islands, yielding Co_9S_8, occurred after extended exposure to the sulfidation mixture. Furthermore, they also observed that the sulfidation of metallic Co occurred at a slower rate than that of CoO.

Thus, our results could be explained by the fact that the presence of hydrogen in the activating mixture enhances the formation of less sulfidable Co species.

Since most of the time the Mo/Al ratio is higher in the Co–Mo catalysts than in the Mo one, when Co is present molybdenum must have a lower tendency to form either larger crystallites or groups with a higher number of slabs. In this way, the coverage of the carrier by the molybdenum sulfide is more extensive. This effect was also observed by Yoshimura *et al.* (51) and by Cruz-Reyes *et al.* (60). The latter also showed that the insertion of Co in bulk MoS_2 induced some disorder in the arrangement of the MoS_2 slabs. Ratnasamy and Sivasanker (31) referred that there is experimental evidence that, already in the oxide phase, Co suppresses the crystalline MoO_3 formation in Co–Mo catalysts.

There seems to exist a general agreement in the literature in that the presence of Co in the Mo catalysts favours the hydrogenation of adsorbed sulfur, with its consequent removal as H_2S (2, 38–41, 61–67). This fact was confirmed in our work also. In the activations where H_2S was used in the absence of H_2, a large excess of surface sulfur was detected in the Mo catalysts (S/Mo $\cong$ 4), whereas in the Co–Mo catalysts the ratio was close to the theoretical one (S/Mo $\cong$ 2).

Modification of the Activation Procedure: Influence on the Nature of the Supported Species

In the following paragraphs we will interpret the changes in the XPS parameters induced by the different activation procedures, considering the known roles of hydrogen and hydrogen sulfide. The catalysts activated according to the simultaneous reduction–sulfidation (RS) method will be considered as possessing typical surface structures. The surfaces issuing from the other activations will be compared to them.

S/RS Treatment. Steinbrunn and Lattaud (42), in accordance with the work of Zabala *et al.* (36, 37), suggested that differences in the mode of sulfur adsorption and sulfidation rate, when either H_2S or H_2/H_2S are employed as activating molecules, could lead to different crystallite sizes of the active phase. Consequently, this would bring about a change of the Mo/Al XPS peak intensity ratio. Our results indicate that the sulfidation using H_2S alone leads to the formation of larger crystallites or crystallites with a larger number of MoS_2 slabs (lower Mo/Al ratio). This result also shows that the subsequent treatment with H_2/H_2S has only a weak influence on the dispersion state of the already formed phase.

When a mixture of H_2/H_2S is employed after activating with H_2S, a decrease of the surface sulfur concentration should occur, albeit limited by the presence of H_2S already in the gas phase. The S/Mo ratio should therefore be higher than after the simple RS treatment, as we observed. It is interesting to notice that, this way, it was possible to restore the NO adsorption capacity of the Mo catalyst, even with a S/Mo ratio well above the stoichiometric value. This suggests that the H_2S adsorbed on the NO adsorption sites (on the edge planes of MoS_2 crystallites) can be removed by the hydrogen present in the activating mixture in the second part of the procedure. On the other hand, the H_2S adsorbed on the basal planes of the MoS_2 crystallites, possibly dissociated into bulk-like S_x species like those proposed by Moulijn and co-workers (38–41), would not be removed by the H_2/H_2S treatment and would be responsible for the high S/Mo ratio.

Dumas *et al.* (59) proposed that the presence of hydrogen in an activation mixture can enhance the formation of metallic Co in the early stages of the activation, yielding a higher degree of sintering of the Co phase. When H_2 is absent, Co^0 may still be formed in the first step of the sulfidation process but a higher dispersion state of the oxide phase will be retained because of the fast sulfidation of that metallic cobalt, thus explaining why the Co/Al ratio increases from the RS to the S/RS activations. In the industrial catalyst, as well as in the laboratory prepared Co catalyst, the amount of sulfidable Co must be lower, leading to a constant Co/Al.

R/RS Treatment. The pre-reduction of the catalyst probably transforms most of the MoO_3 into MoO_2 (8, 9, 36), which is not easily sulfided (10, 36, 39). Some authors say that this transformation may destroy the layer structure or provoke the sintering of the patches of dispersed MoO_3, thus yielding a shrinking of the molybdena layer and leading to a higher exposure of the support (10, 68–71). During reduction bulk-like MoO_3 species will pass from an octahedral to a tetrahedral coordination, with possible breaking of oxygen bridging bonds, and polymeric tetrahedral MoO_3 species may lose bridging oxygen atoms that link the different tetrahedra (8, 42).

The sulfidation (RS) of the reduced catalyst is likely to occur only at its outermost surface (maybe only an O–S exchange at the terminal Mo–O bonds) due to the presence of the less sulfidable MoO_2. In this situation, it is probable that the normal dispersion decrease due to the sulfidation, the formation of MoS_2 crystallites, doesn't occur to such a large extent. In its final state, the catalyst will present a dispersion that is higher than that when it is first sulfided with a mixture containing hydrogen sulfide, although the sulfur concentration will be lower than that resulting from other activation procedures.

In the oxide catalysts, the cobalt that did not interact with the alumina carrier is prone to be fully transformed into metallic cobalt during the initial reduction step of the activation (36, 38, 40, 59). This reduction to Co^0 can be accompanied by sintering. Since Co^0 is easily sulfidable

(36, 40, 59), a subsequent treatment with a mixture of hydrogen/hydrogen sulfide will transform it into Co_9S_8, however its dispersion state will be lower than when it is directly sulfided. This explains the decrease of the Co/Al ratio of the laboratory prepared Co–Mo catalyst when compared to the standard RS procedure. This behaviour was also mentioned in (72), where the authors proposed, apart from Co sintering, its migration to positions beneath Mo. This effect could be partly compensated by the Co surface concentration increase due to the sulfidation, as proposed by Okamoto *et al.* (73).

The different behaviour of the industrial Co–Mo catalyst is certainly due to differences in the surface concentration of reducible/sulfidable Co, and to differences in the interaction degree existing between the Co and Mo phases already in the oxide phase. This may be the reason why in (65) it is reported that a surface Co enriching occurs when pre-reducing Co–Mo/Al_2O_3 catalysts, unlike what we mentioned above.

RS/S Treatment. A H_2S treatment of the sulfided catalysts may increase the amount of detected sulfur at the surface of the catalysts, possibly due to a dissociative chemisorption of H_2S on special sites of the active phases. The observed increase of the S/Mo ratio, for the post-sulfided (RS/S) catalysts, suggests that H_2S may remain adsorbed on the surface of the catalyst after the activation. Furthermore, since the value obtained is higher than the stoichiometric one, especially for the Mo catalyst, the existence of sulfur species other than those pertaining to molybdenum sulfide, is probable.

It is interesting to realise that the presence of Co in the Co–Mo catalysts led to a marked decrease of the S/Mo ratio, when compared to the Mo catalysts, even though the NO adsorption characteristics remained the same in both types of catalysts. This means that the availability of NO adsorption sites is regulated by the H_2/H_2S ratio in the gas phase, whereas the surface sulfur concentration is mainly affected by the presence of Co in the catalyst.

RS/R Treatment. Temperature-programmed reduction studies of sulfided catalysts (38) have shown that the complete reduction of the catalyst's sulfided phase occurs only at temperatures higher than the ones we employed in the activation of the catalysts. Therefore, no reduction nor major phase transformations are to be expected when the catalysts are post-reduced, as in the RS/R treatment. This is confirmed by the absence of Mo^0 lines in the XPS spectra (we recall here that if Co^0 existed it would not be possible to clearly differentiate it from Co_9S_8 using XPS alone). Startsev *et al.* (62) mentioned that the Mo–S bond is more stable than the Co–S one so that Co sulfide may eventually be reduced to Co^0 whereas MoS_2 will not.

Since the S/Mo ratio is still close to the stoichiometric ratio a high degree of sulfidation probably exists. However, the sulfur content of the catalysts diminished, certainly due to the exposure to a reducing atmosphere. Labile sulfur species present at the surface of the catalysts or even fewer strongly bound sulfur anions (from the Mo or Co sulfided phases) may have been hydrogenated and desorbed as hydrogen sulfide. There is also the possibility that the treatment with pure hydrogen will lead to an enrichment of the surface in hydrogen, possibly via the formation of S–H bonds (74) or others, although this effect cannot be detected by XPS.

The removal of sulfur from the catalysts during post-reduction could lead to the formation of larger particles, via sintering due to crystal structure rearrangements, as suggested by Kalthod and Weller (75). This would explain the decrease of the Mo/Al and Co/Al ratios we observed by post-reducing the Mo-containing laboratory-prepared catalysts.

CONCLUSIONS

The modification of the standard simultaneous reduction–sulfidation (RS) activation procedure influences the final distribution of the supported species, especially the diameter of the MoS_2 crystallites and probably that of the Co_9S_8 ones. This effect was clearly identified in the case of the monometallic catalysts, whereas in the case of the bimetallic ones it was blurred by the mutual interference of Co and Mo on each other's dispersion.

The sulfidation of the catalysts with H_2S alone leads to a decrease of the coverage of the support by the molybdenum sulfide phase which can be attributed to a larger crystallite diameter. The pre-reduction of the catalysts leads to a generalised decrease of the amount of surface sulfur, attributed to the difficult sulfidation of MoO_2 formed during the reduction step of the catalyst. A sintering of the Co phase during reduction can be proposed as an explanation for the decrease of its dispersion. The post-treatment of the sulfided catalysts does not cause changes as deep as the pre-treatments do. Nevertheless, the amount of surface sulfur increases or decreases as hydrogen sulfide or hydrogen are used, respectively.

The incorporation of Co in the Mo catalyst leads to an increase of the dispersion of the former, to its higher sensitivity to the activation procedures, and to an increase of its sulfided or reduced phase. Upon sulfidation, the dispersion of the Mo phase does not diminish as much as with the monometallic catalyst. Finally, a general decrease in the amount of surface sulfur can then be detected. We attribute the latter effect to an enhanced rate of reduction of surface sulfur due to the presence of Co.

ACKNOWLEDGMENTS

The authors thank Mr. Michel Genet for the helpful discussions concerning the XPS work and results. They also acknowledge the financial support from "Services de Programmation de la Politique Scientifique—SPPS," Belgium.

REFERENCES

1. Gissy, H., Bartsch, R., and Tanielian, C., *J. Catal.* **65,** 158 (1980).
2. Gissy, H., Bartsch, R., and Tanielian, C., *J. Catal.* **65,** 150 (1980).
3. Prada Silvy, R., Fierro, J. L. G., Grange, P., and Delmon, B., *in* "Preparation of Catalysts IV" (B. Delmon, P. Grange, P. A. Jacobs, and G. Poncelet, Eds.), p. 605. Elsevier, Amsterdam, 1987.
4. Prada Silvy, R., Grange, P., and Delmon, B., *in* "Actas X Simpósio Iberoamericano de Catálise, Mérida, Venezuela, 1986," p. 407.
5. Yamada, M., Shi, Y.-L., Obara, T., and Sakaguchi, K., *J. Jpn. Pet. Inst.* **33**(4), 227 (1990).
6. Pirotte, D., Grange, P., and Delmon, B., *in* "Proceedings, 4th International Symposium on Heterogeneous Catalysis, Varna, Bulgaria, 1979," Vol. 2, p. 127.
7. Delmon, B., *in* Proceedings, Climax 3rd International Conference on Chemical Uses of Molybdenum" (H. F. Barry and P. C. H. Mitchell, Eds.), p. 73. Climax Molybdenum Co., Ann Arbor, MI, 1979.
8. Zingg, D. S., Makovsky, L. E., Tischer, R. E., Brown, F. R., and Hercules, D. M., *J. Phys. Chem.* **84,** 2898 (1980).
9. Li, C. P., and Hercules, D. M., *J. Phys. Chem.* **88,** 456 (1984).
10. Okamoto, Y., Tomioka, H., Katoh, Y., Imanaka, T., and Teranishi, S., *J. Phys. Chem.* **84**(14), 1833 (1980).
11. Alstrup, I., Chorkendorff, I., Candia, R., Clausen, B. S., and Topsøe, H., *J. Catal.* **77,** 397 (1982).
12. Hall, W. K., *in* "Proceedings, Climax 3rd International Conference on Chemical Uses of Molybdenum" (H. F. Barry and P. C. H. Mitchell, Eds.), p. 244. Climax Molybd. Co., Ann Arbor, MI, 1982.
13. Hayden, T. F., and Dumesic, J. A., *J. Catal.* **103,** 366 (1987).
14. Delannay, F., *Appl. Catal.* **16,** 135 (1985).
15. Leyrer, J., Mey, D., and Knözinger, H., *J. Catal.* **124**(2), 349 (1990).
16. Brinen, J. S., and Armstrong, W. D., *J. Catal.* **54,** 57 (1978).
17. Leyrer, J., Zaki, M. I., and Knözinger, H., *J. Phys. Chem.* **90,** 4775 (1986).
18. Brown, J. R., and Ternan, M., *Ind. Eng. Chem. Prod. Res. Dev.* **23,** 557 (1984).
19. Declerck-Grimee, R. I., Canesson, P., Friedman, R. M., Fripiat, J. J., *J. Phys. Chem.* **82**(8), 885 (1978).
20. Declerck-Grimee, R. I., Canesson, P., Friedmann, R. M., and Fripiat, J. J., *J. Phys. Chem.* **82**(8), 889 (1978).
21. Brown, J. R., McIntyre, N. S., Johnston, D., and Coatsworth, L. L., *SIA, Surf. Interface Anal.* **9**(1–6), 255 (1986).
22. Chin, R. L., and Hercules, D. M., *J. Phys. Chem.* **86,** 3079 (1982).
23. Prada Silvy, R., Thesis, Louvain-la-Neuve, 1987.
24. Okamoto, Y., Adachi, T., Nagata, K., Odawara, M., and Imanaka, T., *Appl. Catal.* **73,** 249 (1991).
25. Gajardo, P., Grange, P., and Delmon, B., *J. Catal.* **63,** 201 (1980).
26. Apecetche, M. A., Houalla, M., and Delmon, B., *SIA, Surf. Interface Anal.* **3**(2), 90 (1981).
27. Ratnasamy, P., and Knözinger, H., *J. Catal.* **54,** 155 (1978).
28. Gour, P. K., Tiwari, J. S., Upadhyay, S. N., Pande, S., Ghosh, P. K., Bhattacharyya, N. B., and Sen, S. P., *in* "Proceedings, Climax 3rd International Conference on Chemical Uses of Molybdenum" (H. F. Barry and P. C. H. Mitchell, Eds.), p. 367. Climax Molybd. Co., Ann Arbor, MI, 1982.
29. Delannay, F., Haeussler, E. N., and Delmon, B., *J. Catal.* **66,** 469 (1980).
30. Wivel, C., Clausen, B. S., Candia, R., Mørup, S., and Topsøe, H., *J. Catal.* **87,** 497 (1984).
31. Ratnasamy, P., and Sivasanker, A., *Catal. Rev. Sci. Eng.* **22**(3), 401 (1980).
32. Topsøe, N.-Y., Topsøe, H., Sørensen, O., Clausen, B. S., and Candia, R., *Bull. Soc. Chim. Belg.* **93**(8–9), 727 (1984).
33. van der Kraan, A. M., Crajé, M. W. J., Gerkema, E., Ramselaar, W. L. T. M., and de Beer, V. H. J., *Appl. Catal.* **39,** L7 (1988).
34. Topsøe, H., and Clausen, B. S., *Appl. Catal.* **25,** 273 (1986).
35. Topsøe, H., Clausen, B. S., Candia, R., Wivel, C., and Mørup, S., *J. Catal.* **68,** 433 (1981).
36. Zabala, J. M., Grange, P., and Delmon, B., Preprints IV Simpósio Iberoamericano de Catalisis, México, Nov. 1974.
37. Zabala, J. M., Grange, P., and Delmon, B., *C.R. Seances Acad. Sci. Sér. C,* **279,** 725 (1974).
38. Scheffer, B., Dekker, N. J. J., Mangnus, P. J., and Moulijn, J. A., *J. Catal.* **121,** 31 (1990).
39. Arnoldy, P., van den Heijkant, J. A. M., de Bok, G. D., and Moulijn, J. A., *J. Catal.* **92,** 35 (1985).
40. Arnoldy, P., de Booys, J. L., Scheffer, B., and Moulijn, J. A., *J. Catal.* **96,** 122 (1985).
41. Scheffer, B., de Jonge, J. C. M., Arnoldy, P., and Moulijn, J. A., *Bull. Soc. Chim. Belg.* **93**(8–9), 751 (1984).
42. Steinbrunn, A., and Lattaud, C., *Surf. Sci.* **155,** 279 (1985).
43. Laine, J., Severino, F., and Golding, R., *J. Chem. Technol. Biotechnol. A,* **34,** 387 (1984).
44. van Veen, J. A. R., Wit, H. D., Emeis, C. A., and Hendriks, P. A. J. M., *J. Catal.* **107,** 579 (1987).
45. Shirley, D. A., *Phys. Rev.* **35,** 4709 (1972).
46. Scofield, J. H., *J. Electron. Spectrosc. Relat. Phenom.* **8,** 129 (1976).
47. Briggs, D., and Seah, M. P., Eds., "Practical Surface Analysis Vol. 1—Auger and X-Ray Photoelectron Spectroscopy" 2nd ed. Wiley, New York, 1990.
48. Portela, L., Thesis, Université Catholique de Louvain, Louvain-la-Neuve, Belgium, 1993.
49. Nag, N. K., *J. Phys. Chem.* **91,** 2324 (1987).
50. Massoth, F. E., Muralidhar, G., and Shabtai, J., *J. Catal.* **85,** 53 (1984).
51. Yoshimura, Y., Matsubayashi, N., Sato, T., Shimada, H., and Nishijima, A., *Appl. Catal. A: General,* **79,** 145 (1991).
52. Qin, X., Xiexian, G., Prada Silvy, R., Grange, P., and Delmon, B., "Proceedings, 9th International Congress on Catalysis, Calgary, Canada, 1988" (M. J. Phillips and M. Turnan, Eds.), Vol. 1, p. 66. Chem. Institute of Canada, Ottawa, 1988.
53. Portela, L., Grange, P., and Delmon, B., "Proceedings, 10th International Congress on Catalysis Badapest, 1992," (L. Guzi *et al.*, Eds.), p. 559. Adadémiai Kaidó, Budapest, 1993.
54. Kasztelan, S., Grimblot, J., Bonnelle, J. P., Payen, E., Toulhoat, H., and Jacquin, Y., *Appl. Catal.* **7,** 91 (1983).
55. Delannay, F., Gajardo, P., Grange, P., and Delmon, B., *J. Chem. Soc., Faraday 1* **76,** 988 (1980).
56. Massoth, F. E., and Zeuthen, P., *J. Catal.* **145,** 216 (1994).
57. Bachelier, J., Tilliette, M. J., Cornac, M., Duchet, J. C., Lavalley, J. C., and Cornet, D., *Bull. Soc. Chim. Belg.* **93**(8–9), 743 (1984).
58. Steinbrunn, A., and Bordignon, M., *Bull. Soc. Chim. Belg.* **96**(11–12), 941 (1987).
59. Dumas, P., Steinbrunn, A., and Colson, J. C., *Thin Solid Films* **79,** 267 (1981).
60. Cruz-Reyes, J., Avalos-Borja, M., Farías, M. H., and Fuentes, S., *J. Catal.* **137,** 232 (1992).
61. DeCanio, E. C., and Storm, D., *J. Catal.* **130,** 653 (1991).
62. Startsev, A. N., Burmistrov, V. A., and Yermakov, Yu. I., *Appl. Catal.* **45,** 191 (1988).
63. Duben, A. J., *J. Phys. Chem.* **82**(3), 348 (1978).
64. McCarty, K. F., and Schrader, G. L., *J. Catal.* **103,** 261 (1987).

65. Korányi, T. I., de Vries, G., and Paál, Z., *Bull. Soc. Chim. Belg.* **96**(11–12), 997 (1987).
66. Okamoto, Y., Nakano, H., Shimokawa, T., Imanaka, T., and Teranishi, S., *J. Catal.* **50,** 447 (1977).
67. Upton, B. H., Chen, C. C., Rodriguez, N. M., and Baker, R. T. K., *J. Catal.* **141,** 171 (1993).
68. Fransen, T., van der Meer, O., and Mars, P., *J. Catal.* **42,** 79 (1976).
69. O'Young, C.-L., Yang, C.-H., DeCanio, S. J., Patel, M. S., and Storm, D. A., *J. Catal.* **113,** 307 (1988).
70. Segawa, K.-I., and Hall. W. K., *J. Catal.* **77,** 221 (1982).
71. Prada Silvy, R., Beuken, J. M., Fierro, J. L. G., Bertrand, P., and Delmon, B., *SIA, Surf. Interface Anal.* **8,** 167 (1986).
72. Yamada, M., and Obara, T., *J. Jpn. Pet. Inst.* **33**(4), 221 (1990).
73. Okamoto, Y., Shimokawa, T., Imanaka, T., and Teranishi, S., *J. Catal.* **57,** 153 (1979).
74. Sundberg, P., Moyes, R. B., and Tomkinson, J., *Bull. Soc. Chim. Belg.* **100**(11–12), 967 (1991).
75. Kalthod, D. G., and Weller, S. W., *J. Catal.* **95,** 455 (1985).